Coastal Engineering 58 (2011) 119–130

Contents lists available at ScienceDirect

Coastal Engineering

journal homepage: www.elsevier.com/locate/coastaleng

Prediction and assimilation of surf-zone processes using a Bayesian network Part I: Forward models

Nathaniel G. Plant [a,*], K. Todd Holland [b]

[a] U.S. Geological Survey, 600 4th St. S., St. Petersburg, FL 33701, USA
[b] Naval Research Laboratory, Stennis Space Center, MS 39529, USA

ARTICLE INFO

Article history:
Received 9 October 2009
Received in revised form 27 August 2010
Accepted 3 September 2010

Keywords:
Wave height
Bathymetry
Field data
Duck94

ABSTRACT

Prediction of coastal processes, including waves, currents, and sediment transport, can be obtained from a variety of detailed geophysical-process models with many simulations showing significant skill. This capability supports a wide range of research and applied efforts that can benefit from accurate numerical predictions. However, the predictions are only as accurate as the data used to drive the models and, given the large temporal and spatial variability of the surf zone, inaccuracies in data are unavoidable such that useful predictions require corresponding estimates of uncertainty. We demonstrate how a Bayesian-network model can be used to provide accurate predictions of wave-height evolution in the surf zone given very sparse and/or inaccurate boundary-condition data. The approach is based on a formal treatment of a data-assimilation problem that takes advantage of significant reduction of the dimensionality of the model system. We demonstrate that predictions of a detailed geophysical model of the wave evolution are reproduced accurately using a Bayesian approach. In this surf-zone application, forward prediction skill was 83%, and uncertainties in the model inputs were accurately transferred to uncertainty in output variables. We also demonstrate that if modeling uncertainties were not conveyed to the Bayesian network (i.e., perfect data or model were assumed), then overly optimistic prediction uncertainties were computed. More consistent predictions and uncertainties were obtained by including model-parameter errors as a source of input uncertainty. Improved predictions (skill of 90%) were achieved because the Bayesian network simultaneously estimated optimal parameters while predicting wave heights.

Published by Elsevier B.V.

1. Introduction

The coastal environment is characterized by extreme variability. Physical variables that exhibit significant spatial and temporal evolution include waves, currents, and bathymetry. This is particularly true in the surf zone, where waves transition from non-breaking to breaking conditions, transferring momentum to drive currents, sediment transport, and bathymetric change. Numerous numerical geophysical models are available that make predictions of these processes. These process models can also be inherently statistical, wherein only quantities that are formally averaged over several wave periods (and, often, averaged over the water column) are simulated. For instance, temporally averaged statistical properties of waves can be accurately predicted by SWAN (Simulating Waves Nearshore, Booij et al., 1999; Ris et al., 1999) given accurate bathymetry, water levels, description of the frequency-directional spectra at boundary conditions, and specification of a number of tuning parameters. Similarly, wave-averaged currents can be predicted by models such as Delft-3D (Lesser et al., 2004; Reniers et al., 2007) or ADCIRC (Westerink et al., 2008) that have clearly demonstrated predictive skill. At higher resolution, wave-resolving Boussinesq models also have excellent predictive skill (Chen et al., 2003) and an ability to simulate at the shorter time scales given correspondingly high-resolution time-series data on the model boundaries. This increased fidelity may be necessary for predicting sediment transport and bathymetric evolution (Henderson et al., 2004). However, the higher temporal resolution of Boussinesq models comes with increased computational cost along with the more demanding specification of boundary conditions.

At the present level of hydrodynamic modeling capability, improved predictive skill typically depends on improving the accuracy of model-boundary conditions (Plant et al., 2009), rather than on refinements of the model parameterizations, indicating that the geophysical theory governing nearshore processes is relatively mature. Modeling of sediment-transport processes is an exception to this statement, where skillful predictions can depend strongly on choice of model parameterization (Ruessink et al., 2007). Parameter dependence is primarily due to the use of wave-averaged models that do not resolve physically important processes such as the details of the wave boundary layer and higher-than-second-order moments of the near-bed velocities (Henderson et al., 2004; Hsu et al., 2006).

* Corresponding author. Tel.: +1 727 803 8747x3072; fax: +1 727 803 2032.
E-mail addresses: nplant@usgs.gov (N.G. Plant), todd.holland@nrlssc.navy.mil (K.T. Holland).

0378-3839/$ – see front matter. Published by Elsevier B.V.
doi:10.1016/j.coastaleng.2010.09.003

Report Documentation Page

Form Approved
OMB No. 0704-0188

1. REPORT DATE	2. REPORT TYPE	3. DATES COVERED
SEP 2010		

4. TITLE AND SUBTITLE	5a. CONTRACT NUMBER
Prediction And Assimilation Of Surf-zone Processes Using A Bayesian Network Part I: Forward Models	5b. GRANT NUMBER
	5c. PROGRAM ELEMENT NUMBER
6. AUTHOR(S)	5d. PROJECT NUMBER
	5e. TASK NUMBER
	5f. WORK UNIT NUMBER
7. PERFORMING ORGANIZATION NAME(S) AND ADDRESS(ES) **Naval Research Laboratory,Stennis Space Center,MS,39529**	8. PERFORMING ORGANIZATION REPORT NUMBER
9. SPONSORING/MONITORING AGENCY NAME(S) AND ADDRESS(ES)	10. SPONSOR/MONITOR'S ACRONYM(S)
	11. SPONSOR/MONITOR'S REPORT NUMBER(S)

12. DISTRIBUTION/AVAILABILITY STATEMENT
Approved for public release; distribution unlimited.

13. SUPPLEMENTARY NOTES
The original document contains color images.

14. ABSTRACT

Prediction of coastal processes, including waves, currents, and sediment transport, can be obtained from a variety of detailed eophysical-process models with many simulations showing significant skill. This capability supports a wide range of research and applied efforts that can benefit from accurate numerical predictions. However, the predictions are only as accurate as the data used to drive the models and, given the large temporal and spatial variability of the surf zone, inaccuracies in data are unavoidable such that useful predictions require corresponding estimates of uncertainty. We demonstrate how a Bayesian-network model can be used to provide accurate predictions of wave-height evolution in the surf zone given very sparse and/or inaccurate boundary-condition data. The approach is based on a formal treatment of a data-assimilation problem that takes advantage of significant reduction of the dimensionality of the model system. We demonstrate that predictions of a detailed geophysical model of the wave evolution are reproduced accurately using a Bayesian approach. In this surf-zone application, forward prediction skill was 83%, and uncertainties in the model inputs were accurately transferred to uncertainty in output variables. We also demonstrate that if modeling uncertainties were not conveyed to the Bayesian network (i.e., perfect data or model were assumed), then overly optimistic prediction uncertainties were computed. More consistent predictions and uncertainties were obtained by including model-parameter errors as a source of input uncertainty. Improved predictions (skill of 90%) were achieved because the Bayesian network simultaneously estimated optimal parameters while predicting wave heights.

15. SUBJECT TERMS

16. SECURITY CLASSIFICATION OF:			17. LIMITATION OF ABSTRACT	18. NUMBER OF PAGES	19a. NAME OF RESPONSIBLE PERSON
a. REPORT **unclassified**	b. ABSTRACT **unclassified**	c. THIS PAGE **unclassified**		**119**	

Standard Form 298 (Rev. 8-98)
Prescribed by ANSI Std Z39-18

These neglected details must be absorbed into the available free parameters. The bottom line is that the predictive skill of the present modeling capability will largely depend on uncertainties in model inputs, model parameters, or both.

Finally, real-world implementation of coastal-process models, useful to emergency managers, the military, lifeguards, and beach-goers who need to make decisions based on rapid environmental forecasts, is becoming a necessity. In this scenario, the fidelity of boundary and initial conditions required by numerical models may be so poor that the inadequacies of the input data can only be improved by additional (and often costly) observations of processes in the interior of the model domain. This sets up a complex situation where optimal solutions require the use of some sort of assimilation model to (1) map incomplete and inaccurate data to the boundary conditions, (2) correct model errors in the interior of the domain, and (3) extend intrinsic model outputs (e.g., wave height) to related observables (e.g., video or radar observations, Bell, 1999; van Dongeren et al., 2008) that can contribute to model improvement. Presently, formal data-assimilation schemes that have been applied to nearshore coastal processes have focused primarily on scientific evaluation of model physics (Feddersen et al., 2004), studying the sensitivity of inverse solutions to the scale of variability (Kurapov et al., 2007), and evaluating unknown model parameters (Plant et al., 2004; Ruessink et al., 2007), rather than to solving the operational problem of inadequate boundary conditions.

The lack of regularly applied data assimilation to nearshore coastal models is likely due to computational constraints of the state-of-the-art models, which often perform simulations at computational times that exceed the simulation time. Furthermore, the coupled wave, current, and sediment-transport problem is nonlinear and requires significant model iteration to converge toward the best inverse solutions (Kurapov et al., 2007). To get an idea for the dimensionality of the problem, consider a coastal region that might span 100 km^2, with a model resolution of 100 m^2, which requires evaluation at 1 million grid positions. At each position, there may be roughly 10 variables of interest (e.g., depth, wave height, energy dissipation, etc.). The models might have a time step of 1 s, and a forecast would estimate hourly averaged conditions requiring evaluation of a total of 10^{10} values to describe the coastal environment. A typical assimilation scheme might require 10 iterations, pushing the total bookkeeping load to 10^{11} values per coastal-process forecast.

Although formal data assimilation is possible, its implementation is difficult in coastal and surf-zone environments because (1) it is computationally intensive; (2) it requires specification of often unknown quantities (such as the model error); (3) it is unwieldy in the face of a large number of uncertainties; and (4) it is unmanageable in the face of a large number of observations. Nonetheless, in practical applications of coastal prediction, forecasts will be expected even from boundary and forcing data with substandard accuracy (e.g., outdated bathymetric survey and hydrodynamic observations, or forecasts with significant uncertainty). At a minimum, model initialization will require some form of data assimilation to correct the imperfect model inputs. For instance, data interpolation of one form or another is a commonly used (and abused) form of data assimilation (Ooyama, 1987; Plant et al., 2002). Regardless of approach, practical applications can be supported only if the data-assimilation method offers some reduction in observation and model errors and, most importantly, provides a useful estimate of prediction uncertainties.

In this two-part paper, we present a new application of Bayesian statistical modeling to surf-zone modeling and assimilation. Part I is devoted to describing the modeling framework and applying it to several case studies focused on forward modeling. Part II is devoted to inverse problems and extending the framework to a very flexible set of assimilation problems. We continue with Part I in Section 2 (Model formulation) by reviewing Bayes Rule and then developing a specific application for surf-zone wave modeling. In Section 3 (Application), we describe a data set used for training the Bayesian network and provide hindcast and forecast prediction examples. These examples highlight the role that data and model uncertainty play in affecting prediction errors. Lastly, in Section 4 (Discussion), we explore the problem of obtaining required uncertainty estimates and demonstrate their impact on model skill.

2. Model formulation

2.1. Review of Bayes Rule

In contrast to variational data assimilation, mentioned in the previous section, we suggest that a Bayesian-inference approach can be used to combine available measurements with nearshore-process models to make statistically robust forecasts. The Bayesian approach is formally consistent with sensitivity-based variational assimilation (Wikle and Berliner, 2007). Bayes Rule is

$$p\left(F_i \mid O_j\right) = p\left(O_j \mid F_i\right) p(F_i) / p\left(O_j\right), \tag{1}$$

where the left-hand side of Eq. (1) is the updated conditional probability of a particular forecast, F_i, given a particular set of observations, O_j. The forecast might include both initial and boundary conditions. The observations might be obtained near the boundaries or in the interior of the model domain. Variational data assimilation strives to return the conditional mean value of the solution: $\overline{F_j} = \Sigma_i\, p(F_i \mid O_j)\, F_i$. A Bayesian approach is more general and strives to estimate the likelihood of many possible forecasts. The first term on the right-hand side of Eq. (1) is the inverse of the left-hand side and is the likelihood of the observations if the forecast is known. This term can include both model and observation errors. That is, if the model and measurements were error free, then an observation would be likely only if it equaled the forecast value. In reality, there are numerous errors causing spread in the likelihood function.

The next term on the right-hand side of Eq. (1) is the prior probability of each forecast. This is what is known about the problem before new data are available. It might be the result of a prior assimilation cycle or derived from climatology. The mean value obtained from this distribution is equivalent to the "background" or "best-guess" solution used in variational ocean data assimilation (Benett, 2002) or in optimal interpolation (Ooyama, 1987). Finally, the last term is a normalization factor to account for the total likelihood of the observations. In variational data assimilation and optimal interpolation, this term is solved by inverting the data covariance and is often responsible for large computational costs. Here, it is estimated through integration over all forecast possibilities.

A primary advantage to the Bayesian approach to data assimilation is that the probability distribution of the forecast is estimated. This allows for both data and forecast to have non-Gaussian probability distributions, which may be crucial to describing strongly nonlinear nearshore processes. In principle, this means that the Bayesian approach will lead to more accurate forecast statistics, including estimates of the most likely forecast and its uncertainty. A possible disadvantage of the Bayesian approach is that it may increase the dimensionality of the problem. If each F_i is a single forecast with 10^{10} quantities to describe it (i.e., the typical numerical model system mentioned earlier), then the complete Bayesian approach requires that we track the joint probability of these variables against observations, which might also be any of the 10^{10} quantities. The problem would have exploded to a dimension of 10^{100}!

In practice, however, the utility of the Bayesian approach is most evident when the problem of interest can be boiled down to a much-reduced dimensionality. (This statement actually applies to most other data-assimilation schemes, which, for instance, do not attempt

to compute the model–data sensitivity at full resolution, Kurapov et al., 2007.) Here, we will apply three standard approaches to reducing the problem's dimensionality. First, we forecast along a 1-dimensional (1-D) slice of the spatial domain, extending from the shoreline across the width of the surf zone into offshore water depths where waves do not usually break. Second, we consider only a subset of the entire spatial domain by focusing on a relatively few locations of interest. Thirdly, we will consider only a subset of the possible processes in the surf-zone region that we deem most important, specifically wave shoaling and breaking.

2.2. A surf-zone Bayesian model

To test our hypothesis that a Bayesian approach to data assimilation can be exploited in the surf zone, we selected the wave-evolution model described by Thornton and Guza (1983) (hereinafter referred to as TG83), which assumes Rayleigh-distributed wave heights throughout the model domain. Our intent is not to substantiate a particular approach over another—since numerous refinements to this model have been developed—but to emphasize that variations in implementation do not change the essential elements of this data-assimilation example. The inherently 1-D TG83 model predicts the evolution of the root mean square (rms) wave height given estimates at the offshore boundary of the wave height, wave direction, and wave period. The model does not resolve the different directions or frequencies that might contribute to a spectrum of waves, because waves are assumed to be narrowly distributed around a peak period and direction. Thus, we can write the forecast from this model at any location, x_k, as,

$$F_i(x_k) = \{H_k\}_i = funct.(\{h_0, h_1, \ldots, h_k, H_0, \alpha_0, T, \gamma, B\}_i), \tag{2}$$

where h is the water depth, H_0 is the offshore rms wave height, and α_0 is the offshore peak-wave direction. Variables with subscript k are spatially varying. Additional parameters are a peak-wave period (T), a critical wave-breaking criterion (γ), and a breaking efficiency (B). All of the inputs can be considered random variables, because even the model parameters must be estimated from the data (Ruessink et al., 2003). Therefore, the ith solution is obtained from a particular choice of inputs. Fig. 1 shows an example of the spatially extensive (in 1 horizontal dimension) input and outputs of this model.

The waves shoal offshore from the outer sandbar and then begin to break, decreasing in height until they reach the shoreline. The change in the wave-height profile will depend on the offshore wave height, period, direction, and the underlying bathymetry. Using the numerical TG83 model, it is not possible to make a prediction unless all of these variables are known. In particular for our case, the bathymetry must be known at approximately 500 locations in order to provide 1-m model resolution across the domain. The dimensionality of the full model is, $4*500+3$, which includes the spatially varying fields of input bathymetry and output wave height, direction, and dissipation, plus the wave period and two model parameters.

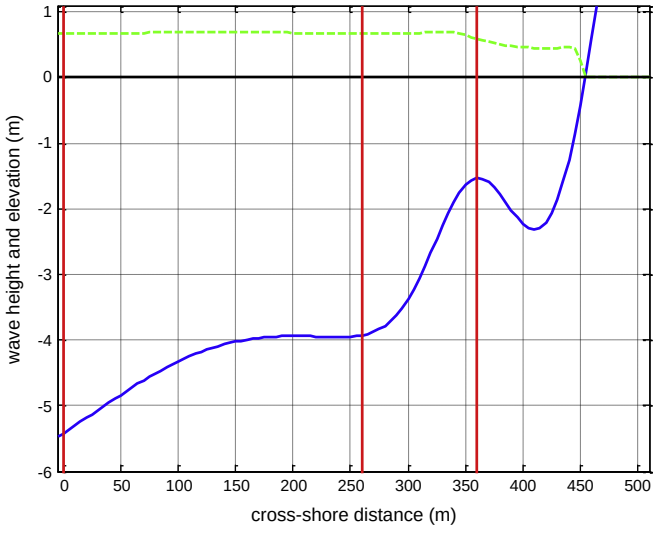

Fig. 1. Wave height (dashed line) simulation over measured bathymetry (solid line). Vertical lines mark reduced Bayesian network's sample locations.

2.3. Reduced model

We expect that the utility of wave-model forecasts does not necessarily rely on providing all of the output predictions possible from the model (O'Reilly and Guza, 1998). For instance, accurate prediction of the wave height very near the beach might be necessary, rather than at all locations in the model domain. Or, if a higher-resolution model is to be initialized from a low-resolution model, only the data at the boundary of the high-resolution model are required. From this point of view, the unused model details are irrelevant. This implies that our data-assimilation problem should only retain a forecast at a small subset of locations. For the surf-zone example, we choose to retain information at our model's boundary, at an intermediate location, and at one location close to the shoreline. We have, in an *ad hoc* way, just reduced the spatial dimensionality from 500 locations to only 3.

The Bayesian versions of this reduced model inputs and outputs are

$$\begin{aligned} F_i &= \{h_0, H_0, h_1, H_1, h_2, H_2, T, \alpha_0, \gamma, B\}_i \\ &\text{and} \\ O_j &= \left\{\hat{h}_0, \hat{H}_0, \hat{h}_1, \hat{H}_1, \hat{H}_2, \hat{h}_2, \hat{T}, \hat{\alpha}_0, \hat{\gamma}, \hat{B}\right\}_j. \end{aligned} \tag{3}$$

The spatial locations are given by subscripts (0 for the offshore boundary, 1 for the intermediate position, and 2 nearshore). A variable with a circumflex indicates that it is an observation (which can be derived from any number of sources, including other models) and the others are predictions. We have included the model parameters γ and B as both observations and predictions. However, without calibration data, these values will be obtained from a prior distribution. Initially, we choose to constrain these parameters to $\gamma = 0.34$ and $B = 0.8$ (Haines and Sallenger, 1994) in order to focus attention on the remaining variables. We will loosen this constraint when we discuss parameter sensitivity later.

A schematic diagram of the Bayesian network representing the reduced model is shown in Fig. 2. This follows a hierarchical approach (Ihlera et al., 2007), which considers only a subset of the total joint correlations that are possible for this system. The network variables are grouped both spatially (from left to right) and by process (top to bottom). The arrows connecting specific variables or groups of variables represent joint correlations between those variables. These correlations will be estimated from measurements or from model predictions as part of the training or calibration process. Although it is entirely possible to represent correlations between each variable and all other variables, we have chosen to take advantage of a further reduction in model dimensionality by representing only a few of the most important correlations (each is labeled with a number). The choice of which correlations to retain is guided by our knowledge of the wave-evolution processes. For example, we know that the wave height at location x_1 depends on the wave height at x_0 (correlation #5), and additional relationships are expected for the water depths at x_0 and x_1 (correlations #7 and #8), wave direction and period (correlation #2), and the model parameters (correlation #4).

In addition, we know that other processes contribute to correlations that would not be represented by the wave model, but would be expressed in the observations. For instance, wave height, direction,

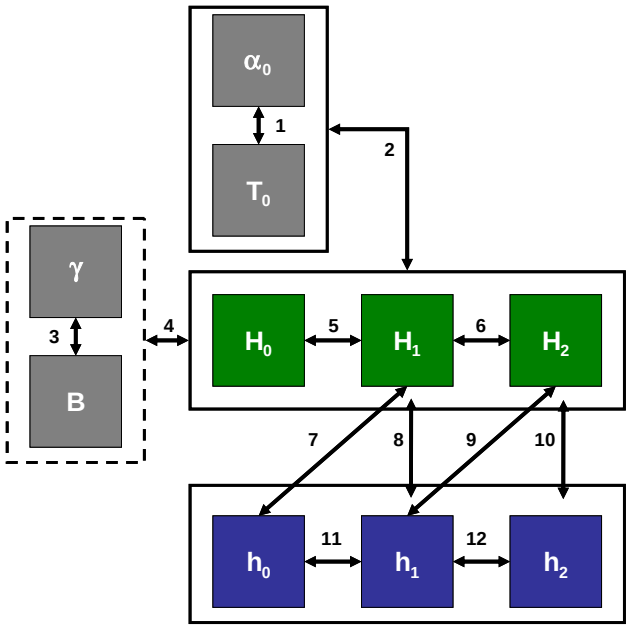

Fig. 2. Surf-zone model representation as a Bayesian network.

and period can be correlated to each other (#1 and #2) due to constraints associated with fetch and storm characteristics. Water depths are correlated to each other (#11 and #12) due to mass conservation and coherent variations associated with sandbars.

The Bayesian network of the reduced model in the assimilation problem has several useful properties, including that it

(1) it achieves a necessary reduction in dimensionality;
(2) it focuses a detailed forecast model on variables and locations of interest;
(3) it estimates forecast uncertainty;
(4) it can be used to inversely estimate boundary conditions for a detailed forecast model (to be shown in Part II); and
(5) it can assimilate diverse inputs, including depth, wave height, wave direction, and dissipation (and more, as we will also show in Part II).

Nonetheless, the Bayesian network still relies on detailed numerical estimates and/or observations because the joint probability that relates $p(F \mid O)$ to $p(O \mid F)$, $p(F)$, and $p(O)$ must be estimated through training based on, essentially, Monte Carlo simulation. The proposed efficiency in the Bayesian approach is in the fact that once all relevant scenarios have been encountered, the detailed numerical model used in the "training" process can be discarded. This is particularly powerful in the nearshore environment where dynamics periodically return to similar beach states (Plant et al., 2006; Wright et al., 1985) and even to identical bathymetric profiles at regular intervals (Ruessink and Kroon, 1994; Wijnberg and Terwindt, 1995). Rather than re-computing the same inputs with a detailed model to get nearly the same outputs, the Bayesian approach stores not only the functional mapping between input and output, but also the uncertainty in the output due to uncertainty in the input.

3. Application

3.1. Bayesian-network discretization

We constructed a representation of Eq. (1) and Eq. (2) with the reduced model Eq. (3) using a numerical implementation of a Bayesian network called Netica (Norsys, 1990–2007). We have already justified the spatial simplifications of the reduced model. An additional level of simplification is required to represent the continuous physical processes with a small number of discrete states. That is, a continuous range of natural wave heights, H, will be represented with a finite distribution of values, H_n, ranging from some minimum value (e.g., 0 m) to a reasonable maximum value (e.g., the maximum observed value or a fraction of deepest water depth, since we know that wave height will be limited to this by breaking). It is not necessary to have constant intervals ($H_{n+1} - H_n \neq H_n - H_{n-1}$). The design of this discretization requires balancing a number of competing interests.

(1) The intervals should be as wide as possible to minimize computational effort.
(2) The intervals should be narrow enough to resolve the expected uncertainty and provide forecast utility. For instance, if the expected rms prediction error were σ_H, then the interval should be no larger than σ_H.
(3) The intervals need to be wide enough to collect at least a few "hits" from the available data and Monte Carlo simulations. The objective is to approximate the joint probabilities of interest by, essentially, compiling histograms. If an interval contains only a small number of samples, the histogram is not well constrained. In practice, we seed all of the joint probabilities with a uniform distribution so that poorly constrained intervals will, at worst, return a uniform distribution as a result.

Constraint #2 suggests that the network resolution should be as detailed as possible while supporting constraints #1 and #3. This is not necessarily the case. There are intrinsic errors, such as model error, that can be easily captured by preventing the intervals from shrinking unnecessarily. Thus, constraint #2 can be interpreted to mean that the intervals should be no finer than about σ_H as well. Additionally, this constraint can be interpreted from a practical point of view, and the interval should be no finer than what is necessary for the appropriate interpretation of the results. For example, an application to beach safety might require only estimating whether the wave height exceeds a critical value. Then, only two bins are required, split at the critical value. We adhere to these design guidelines using an adaptive method, described in the next section.

3.2. Training data set

The proposed Bayesian network could be developed for any arbitrary location. We selected the Army Corps of Engineers Field Research Facility (FRF), in Duck, NC. At this site there is a long time series of bathymetry and wave observations. These data are sufficient to drive a forward model of wave shoaling and breaking corresponding to a large range of prediction scenarios. We emphasize that locations with less extensive data sets could also work within this modeling concept, but that the source data from this location are well established and easy to obtain. Fig. 3 shows histograms of daily-averaged data for the period 1980 to 1996, using essentially the same data set as that analyzed by Plant et al. (1999). The wave data were measured approximately every 3 h. The bathymetry was measured approximately monthly and was interpolated to a daily interval using an objective interpolation scheme. The computational domain of the TG83 mode extended offshore to the 8-m contour where wave data were measured. The measured bathymetry was spatially interpolated to 1-m intervals across the domain. The measured inputs and model parameters (γ and B) were inputted to the TG83 model, and the output wave-height predictions were stored at offshore, intermediate and onshore locations. Note that the purpose of the modeling exercise at this stage is to obtain data to be used to estimate correlations both among and between model inputs and outputs. Although this could be accomplished with synthetic data, the field data set provides accurate prior probabilities for the input and output variables. The interpolation scheme produced smooth results in both space and time and filtered out some short spatial and temporal variability. A potential impact of this is that some wave conditions may be paired with some

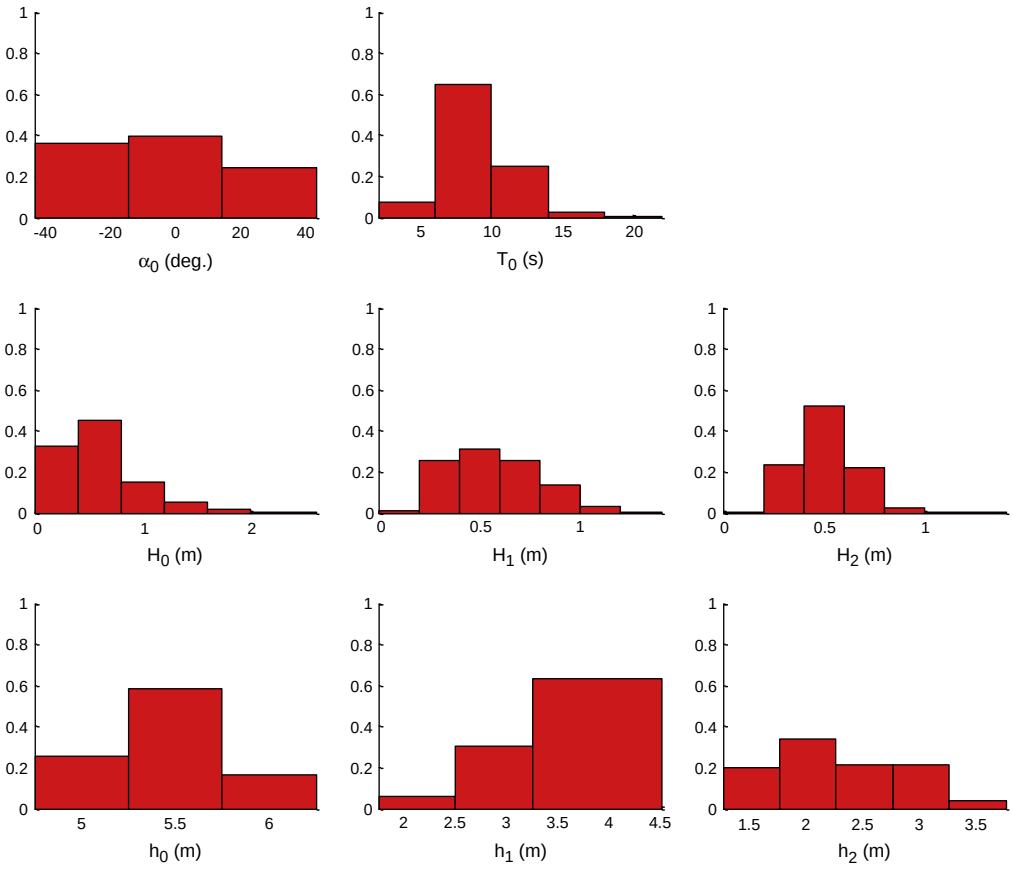

Fig. 3. Prior distributions of Bayesian network's variables.

profile conditions that are not fully consistent with nature. If this problem is significant, new observations may be identified as being inconsistent (highly improbable) or, more likely, this simply adds to predicted uncertainty.

Using the observations and corresponding simulations, we initially assigned minimum bin widths to each variable. These widths were $\sigma_h = 0.25$ m, $\sigma_H = 0.2$ m, $\sigma_T = 2$ s, $\sigma_\alpha = 15°$. The bins were then altered such that each would contain 20% of the data (e.g., five bins if the data were uniformly distributed). If this initial scheme produced bins that were narrower than the minimum value, the bin width was increased such that there might be fewer than five bins for a variable. The histograms shown in Fig. 3 reflect the resolution that resulted using this scheme.

The observation/simulation results were read into Netica, which assimilated these data into tables representing the joint probability of the wave model and input data. Initially, the joint probabilities were given a uniform distribution. Then, these distributions were updated to yield the maximum likelihood probabilities, given the available data. That is, the data were used to solve an inverse model for the Bayesian network itself, treating each joint probability as an unknown parameter. There were 15,435 unknown joint probabilities. These were constrained with 39,037 observed and simulated values. Since we assume that the probabilities of adjacent intervals are somewhat correlated, there is no requirement that the number of inputs exceeds the number of unknown network variables. And, we expect that many scenarios are unlikely (for instance, shallow depths at all locations would not occur), such that the initial uniform distribution adequately initializes these unobserved states. Furthermore, it is possible to assimilate data with missing values for some of the variables. For instance, there were numerous occasions where the wave direction at the offshore boundary was unknown. These cases simply distribute their probability over all possible values of wave direction while constraining the joint probability of the remaining non-missing variables.

3.3. Prediction example

Once the Bayesian network is "trained" on the available observations and simulations, we can use it to make forward and inverse predictions (the latter will be described in Part II). The purpose of the forward prediction is to demonstrate the accuracy of the reduced model relative to the original model as well as to illustrate how degraded or inaccurate input data affect the uncertainty of the output prediction.

3.3.1. Prior prediction

The first example of the Bayesian-network prediction has already been demonstrated in Fig. 3. It is the prior prediction, which is available before we constrain and update the network with specific case data. In this situation, the prior prediction captures our understanding of the likelihood of particular outcomes based on climatology. For instance, some variables actually change very little (e.g., the water depth at the seaward boundary), whereas others are extremely variable (the wave height at the seaward boundary). Data will be compared to this prior set of distributions via Eq. (1). The immediate value of the prior is to identify the consistency of the data. Data that are consistent with the prior will lead to increased certainty for all of the variable's distributions. Data that are inconsistent will result in very uncertain distributions. Thus, the prior is useful for evaluating the quality of the data as well as for updating the predictions.

3.3.2. Forward prediction

The next example of the Bayesian network (Fig. 4) demonstrates its ability to reproduce specific predictions, given data describing

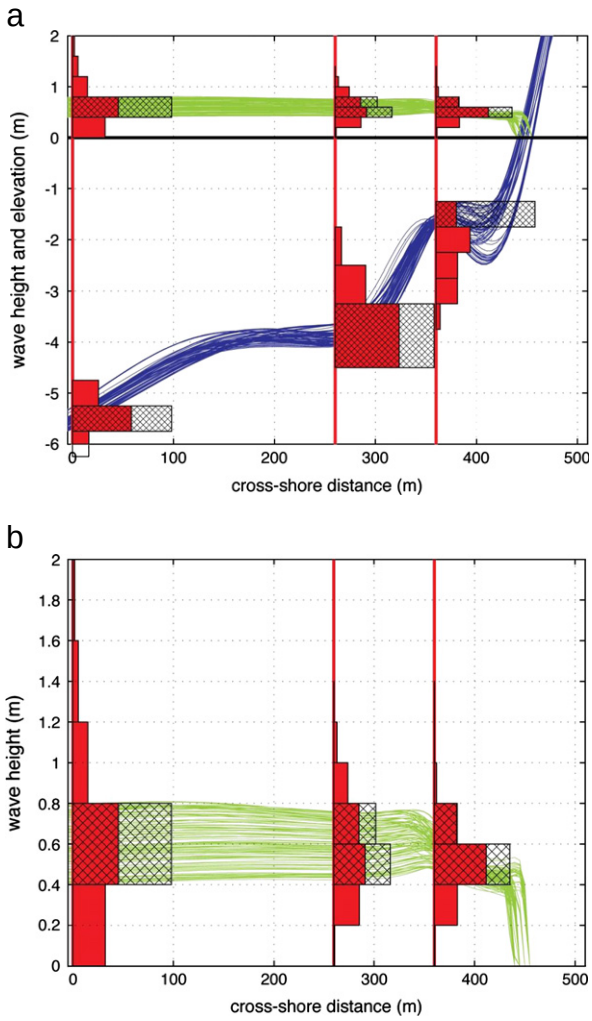

Fig. 4. Comparison of Bayesian network prior prediction (red histograms) and updated prediction (cross-hatched histogram) to (a) detailed input bathymetry (blue lines) and (b) detailed wave shoaling and breaking predictions (green lines).

boundary conditions. Using the Bayesian network, we reproduce the simulations shown in Fig. 4 with offshore wave height known to be in the range of 0.4 to 0.8 m, period of 6 to 10 s, unknown direction, and water-depth distributions centered on 5.5, 3.8, and 1.5 m at the offshore, intermediate, and onshore locations. Given this information, the predicted wave height (shown without bathymetry in Fig. 4b) at the intermediate location is most likely to be in the range of 0.4 to 0.6 m (60% likelihood), but there is some likelihood for values in the range of 0.6 to 0.8 m (40%). At the onshore location, there is more confidence for the 0.4 to 0.6 m range (80%), with the remaining 20% likelihood falling in the 0.6 to 0.8 m range. In all cases, the prediction that was obtained by updating the Bayesian network (black histograms) has a significantly narrower distribution than the prior distribution (red histograms), and the updated predictions are, as expected, more consistent with the results from the TG83 wave model.

The next forward prediction (Fig. 5) replaces the well-constrained input wave height at the offshore boundary with more uncertain information. The input wave height was updated with an input probability distribution that was uniformly distributed over the range of 0 to 1 m. This is meant to illustrate the effects of measurement error or, alternatively, forecast uncertainty if one was initializing the wave model with output from a numerical weather prediction. This example also indicates the utility of having a so-called "informative"

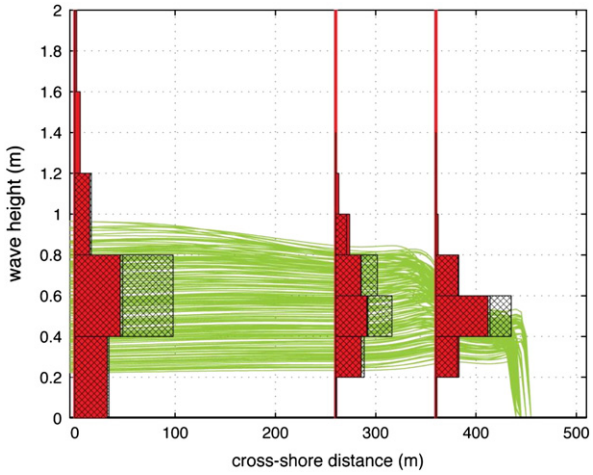

Fig. 5. Comparison of Bayesian prediction with increased offshore wave height uncertainty.

prior distribution. Even though the offshore boundary data were inputted with uniform distributions, the updated probability distributions (Fig. 5) of the offshore wave height are very similar to the priors. The Bayesian network "knows" that moderate wave heights are more likely than either extremely high or low values and corrects the inaccurate input data.

The result of the increased input uncertainty is the increased prediction uncertainty at the landward locations. Specifically, the wave-height prediction at the landward location has degraded to just 50% likelihood for values in the 0.4- to 0.6-m range, compared to 80% likelihood in the previous example. While the prediction uncertainty at the landward-most location has increased, it is clear that the 0.4- to 0.6-m estimate is far more likely than any other value. This result is due to the wave-breaking processes that act to reduce the wave-height variability close to shore. Thus, uncertainty in some input variables does not necessarily have the same impact on all output variables.

The next prediction example (Fig. 6) illustrates the Bayesian networks' ability to identify inconsistent data. In this case, the offshore wave conditions used in the first example were applied, but unlikely depth observations were provided as input (depths at all three locations were set to the shallowest levels with 100% certainty). The result is somewhat degraded certainty of the wave height at the intermediate location (i.e., roughly 50% likelihood for both 0.4- to 0.6- and 0.6- to 0.8-m levels). However, at the onshore location, the wave-height prediction probability is distributed uniformly over all

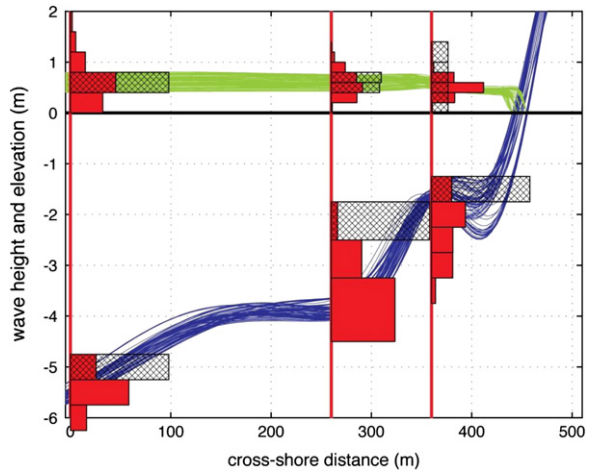

Fig. 6. Prediction with inconsistent depth inputs.

possibilities, which is worse than the uncertainty associated with the prior prediction. This increase in uncertainty indicates that this specific input scenario is one that has no prior information. Either the Bayesian network must be trained to encompass this new (perhaps unrealistic) input, or it demands that the data be inspected for errors.

3.3.3. Field evaluation

The previous examples compared the Bayesian network to the model output and data that were used to train it. This hindcast simply demonstrated how the Bayesian network responds to different types of input and demonstrates that it can recover the detailed TG83 model prediction. Next, we compare the Bayesian predictions to new field observations of surf-zone wave heights. The Bayesian network was not trained with these new surf-zone measurements, relying on the previous training as before.

The new field data were obtained as part of the Duck94 experiment (Birkemeier and Thornton, 1994). We used the data from 17 pressure sensors (Fig. 7) that measured wave heights (Elgar et al., 1997; Gallagher et al., 1998). Bathymetry data were obtained by interpolation of daily surveys. Tides observed on a nearby pier were used to correct the bathymetry to obtain depth estimates appropriate to each observed wave height. As before, the offshore wave conditions and depths at all locations were used to update the Bayesian network and obtain forward predictions of the wave heights at the intermediate and landward locations. We focus the remainder of our analysis on the Bayesian prediction of the wave height at the onshore location only.

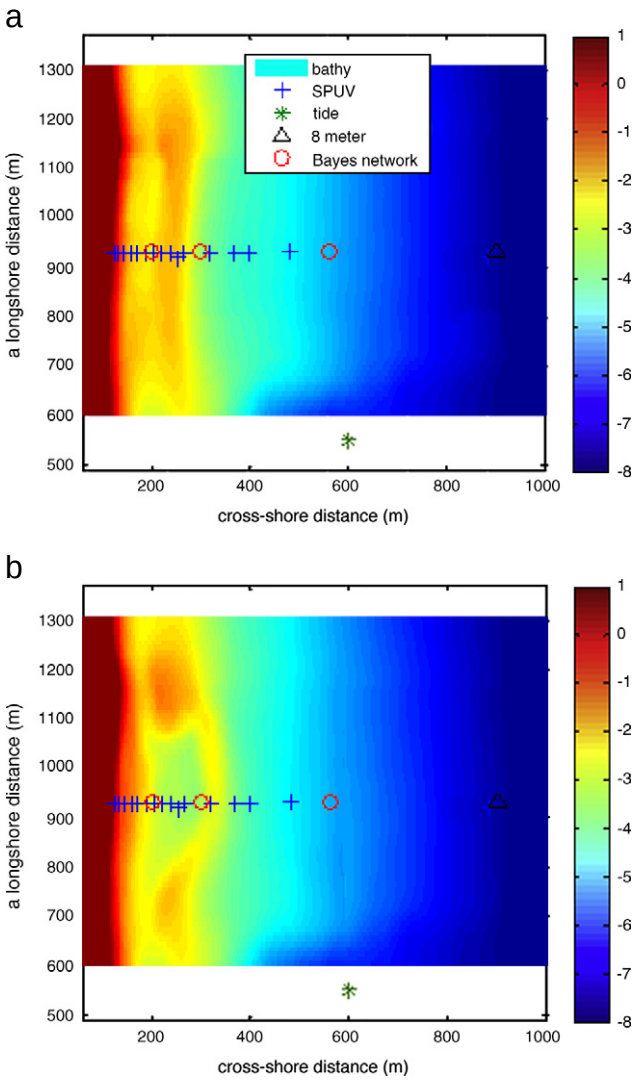

Fig. 7. Instrument locations and bathymetry on (a) 04 and (b) 24 October 1994.

We assume, initially, that all of the data are error free—at least to the level of precision required to specify the Bayesian network's inputs. Fig. 8 shows a comparison of the observed and predicted wave heights at the onshore location. The predictions track the observed wave height variations that are associated with changes in water depth (tide) and offshore wave height. The skill of the Bayesian network's mean prediction is 79% with a mean error of −0.04 m (i.e., an under-prediction) and rms error of 0.15 m. (The skill was defined as $1-\sigma_e^2/\sigma_o^2$, where σ_e^2 mse is the mean-square error between Bayesian predictions and the observations and σ_o^2 is the variance of the observed nearshore wave height.) The most likely prediction has about the same mean and rms errors and skill (−0.05 m, 0.14 m, and 80%, respectively). However, it is clear from Fig. 8 that the prediction skill is not uniformly accurate. During the second half of the time series (when the bathymetric surveys indicated strong alongshore variability), the prediction systematically underestimated the observations. In fact, a more serious error lies in the predicted uncertainty (indicated by the width of the shadings), which does not include the observations and, hence, is under-predicted during the period with the highest waves.

Calculation of wave heights using the original TG83 wave model for this interval shows that the tendency for under-prediction of the highest wave heights is actually an intrinsic numerical modeling error and is not due to the Bayesian re-formulation. We will demonstrate that this systematic error can be reduced by allowing for uncertainty in the model parameters, which have been held constant so far. Fig. 9 shows a comparison of observed and predicted wave heights at the onshore prediction location. The mean prediction error of the wave model (labeled TG83) was −0.03 m; the rms error was 0.07 m, and the prediction skill was 97%. The improved skill and roughly 7 cm of reduced rms error were obtained at the expense of providing the entire bathymetric profile to the TG83 model—rather than just the bathymetry at the three locations required by the reduced Bayesian network—and numerically solving a differential equation for each new set of observations (no matter how slightly they may have changed).

The high-resolution numerical model cannot do anything to identify systematic prediction errors (such as errors associated with the high waves at the end of the study period). On the other hand, we demand that the Bayesian network predicts both best estimate (e.g., mean and most likely) values and uncertainties. The point of tracking uncertainty is to alert users of the predictions to situations when there is a high probability of prediction error. Unfortunately, for the second half of the data set, there is a serious failure in the Bayesian prediction to identify prediction uncertainty because the Bayesian network was, naively, based on an inaccurate wave model.

4. Discussion

4.1. Quantifying Bayesian-prediction skill

The Bayesian-assimilation approach turns the typical model-evaluation procedure on its head. Typically, a model is calibrated to make its best prediction through tuning of parameters in order to fit a hindcast prediction through a cloud of observations. The assumption is that the model–data mismatch will be used to evaluate the probability distribution of tunable parameters and prediction errors. The Bayesian-network prediction already includes the probability distributions. Thus, it is possible to evaluate the network with each independent observation. This is done by evaluating the likelihood of an observation, given the updated prediction. The likelihood is

$$L_j = p\left(F_i|\tilde{O}_j\right)_{F_i=O_j} \tag{4}$$

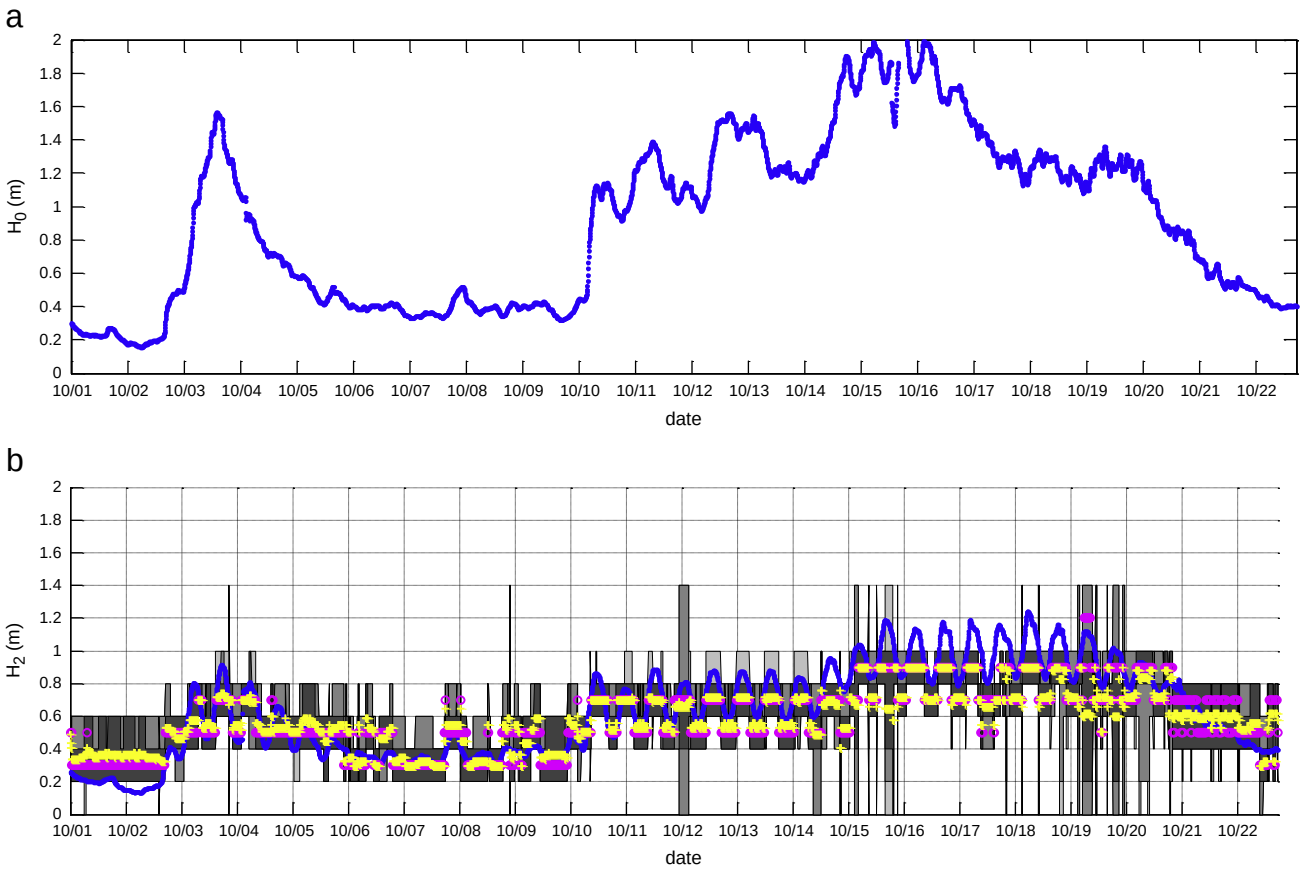

Fig. 8. Observation of (a) offshore wave height and (b) comparison of observations and predictions at the onshore location. The shading indicates the predicted uncertainty with lightest shading for the 95% confidence interval, medium shading for 90% confidence, and dark for the 50% confidence. The blue dots are the observed surf-zone values, and magenta circles indicate the most likely prediction (i.e., the Bayesian-network bin that contains most probability at each sample time). The yellow crosses mark the mean prediction (i.e., the expected value from the Bayesian prediction).

where $\tilde{O}_j$ is the subset of observables that are made available to the Bayesian network for prediction and O'_j is the independent observation that was withheld from the prediction. For instance, $\tilde{O}_j$ might include the bathymetry at all locations as well as the wave height at the offshore location, and O'_j might be the wave height at the onshore location.

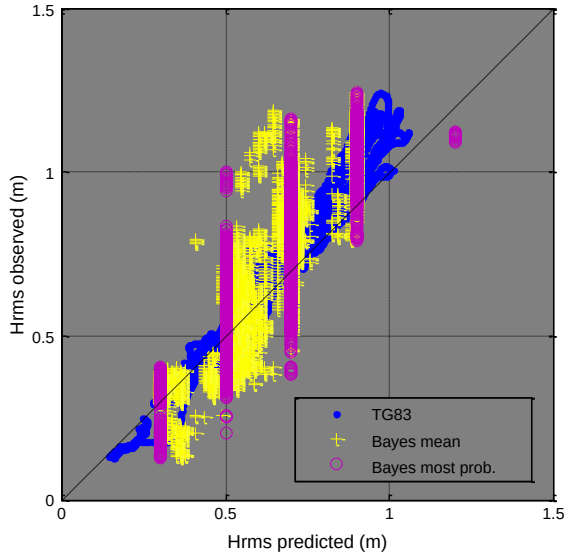

Fig. 9. Comparison of predicted and observed wave heights.

An approach to testing the Bayesian-network prediction is to compare it to a competing model. One such competing model is the prior probability, which is determined before the network is updated with specific observations. If the likelihood of the data is increased under the updated network, then it will have a positive log likelihood ratio:

$$LR_j = \log\left\{p\left(F_i|\tilde{O}_j\right)_{F_i=O'_j}\right\} - \log\left\{p(F_i)_{F_i=O'_j}\right\}. \quad (5)$$

A likelihood ratio exceeding 1 indicates a significant improvement in the prediction. This will result if the Bayesian network confidently predicts a distribution centered on the observation. A ratio less than 0 is worse than the prior prediction. This can result in the case of a confident prediction that misses the verification data (such as the high-wave prediction errors). Thus, the likelihood ratio simultaneously tests the skill of the best prediction (which could be the mean or mode of the distribution) and tests the skill of the uncertainty prediction by penalizing both overly certain and uselessly uncertain predictions.

The likelihood ratio summed over all observations and predictions that are shown in Fig. 8 was −1000. That is, even though the mean predictions were very skillful, the estimate of the uncertainty was not accurate. The uncertainties were overly confident such that the observations were more likely to come from the prior network prediction (which was the same for all sample times) than the updated prediction. One explanation for this is the omission of information about input errors. Particularly important are depth

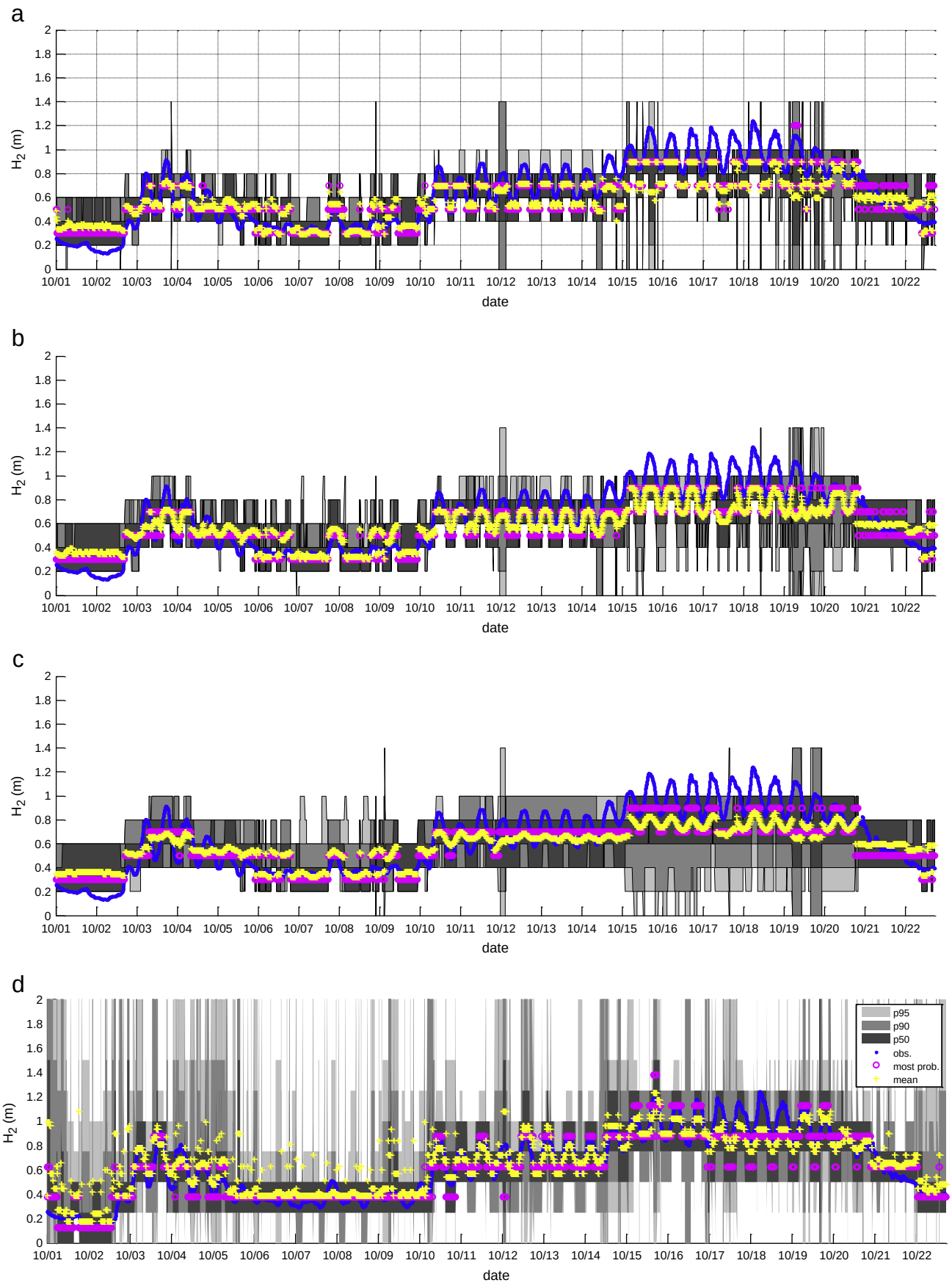

Fig. 10. Comparison of Duck94 observations to predictions for input bathymetric uncertainty equal to (a) 0, (b) 1, and (c) 4 times the true bathymetric uncertainty values. Including wave-parameter uncertainty (d) improves the prediction and leads to more consistent estimates of the uncertainty.

errors and model errors. Depth errors may result from survey inaccuracies and alongshore variability. Since the underlying process model assumed alongshore uniform bathymetry, an obvious solution is to include alongshore variability as an additional measure of uncertainty. Model errors might result from using the wrong model-parameter values.

4.2. Prediction sensitivity to bathymetric uncertainty

To test whether including input uncertainty could improve the likelihood score, we generated input distributions for the depth data from the computed residual errors between survey data near the Duck94 instrument array and the interpolated profile used as input for both the Bayesian and TG83 models. Because the alongshore spacing of survey data was between 25 and 50 m, residuals were computed from the data within 100 m of the alongshore position of the array. This selection of data is somewhat arbitrary, but it balanced a need for sufficient samples to allow calculation of a meaningful residual error, yet still remains focused on the location where the waves were measured. Fig. 10 shows the updated predictions that utilize the input uncertainty, which was assumed to be normally distributed with standard deviations that were, on average, 0.65, 0.15, 0.12 m at the three input locations. The uncertainty in the Bayesian network's predictions changed most in the second half of the time series, which corresponds to the development of a crescentic-bar shape (Fig. 7). The likelihood ratio increased to LR = 300 when bathymetric uncertainty was included, indicating more accurate uncertainty estimation. The error statistics of the Bayesian mean prediction were unchanged.

Since the local alongshore variability might not represent all of the impacts of bathymetry errors and it certainly does not represent the impact of intrinsic modeling errors, it is possible to use bathymetric uncertainty as a tuning parameter to optimize the prediction accuracy. We progressively increased the amount of uncertainty input to the Bayesian network by factors of two and found that the highest likelihood ratio (i.e., the most improvement over the prior prediction) was achieved for input uncertainty equal to 4 times the actual values. The best ratio was LR = 1800. This result indicates that, perhaps, the missing cross-shore detail in the bathymetric variability (due to using a subset of spatial locations) plus the missing alongshore detail (due to the assumption of alongshore uniformity) should be included together in the input uncertainty. Alternatively, the source of prediction error lies elsewhere (e.g., with the model parameters) and the use of unrealistically high depth uncertainty is simply a cover-up for the real problem. In fact, it is clear that a side effect of improving the accuracy of the Bayesian estimate of uncertainty is to reduce the variability of the predicted response. For instance, in Fig. 10c, the mean and most likely predictions do not exhibit a strong tidal modulation for the first half of the record. And, the Bayesian network continues to under-predict the wave height in the second half of the record.

Table 1 summarizes the error statistics of the most landward location for all the updating methods described so far. Three additional methods are included. One, labeled "Onshore H_{rms}", used the measured surf-zone wave height at the onshore prediction location as input to the Bayesian network. That is, we showed the Bayesian network the answer. The purpose of this test is to identify the degraded skill due to the resolution of the probability bins. As the bins became coarser, the network would not adequately resolve the best answer even when that answer was known. In fact, there was very little degradation of the model skill when compared to the TG83 results: skill reduction from 97% to 94%. This test is also a good reference since it indicates the maximum possible likelihood score (= 5683).

The method labeled "No Bathymetry" did not include any bathymetry data as input to the Bayesian prediction—that is, only the prior information from the training on the historical data set was utilized. Only the offshore wave observations were used to make predictions in this case. The method labeled "No Offshore H_{rms}" used the bathymetry observations but did not use the measured wave parameters. Mean and rms errors were highest for the case where the wave-height observations were omitted, indicating that observations of bathymetry were of secondary importance. With no update in bathymetry, the network propagates the known bathymetric uncertainty to the wave-height prediction, scoring well (1483) in the likelihood-ratio test. If the wave height, direction, and period are not updated, the "No Offshore H_{rms}" scenario does not score well in the likelihood-ratio test (−157) and has poor skill (12%). An outcome of this comparison is that we can place relative values on updated bathymetry vs. updated wave observations. In this case, the offshore wave-height data contribute about six times more than the bathymetry data to skill improvement. This result depends, of course, on the duration of the field test, which was long enough to experience a wide range of wave conditions, but shorter than needed to experience the full range of bathymetric states.

Table 1
Error and skill statistics for mean wave height prediction at the onshore location.

Update method	Mean error (m)	RMS error (m)	Skill (%)	Likelihood ratio
TG83 model	−0.03	0.07	97	n/a
No uncertainty	−0.04	0.15	79	−1011
Bathymetric uncertainty				
Uncertainty = 1σ	−0.04	0.15	83	320
Uncertainty = 2σ	−0.04	0.15	83	1386
Uncertainty = 4σ	−0.04	0.16	81	1859
Uncertainty = 8σ	−0.03	0.16	77	1815
No Bathymetry	−0.06	0.20	68	1483
γ uncertainty				
Uncertainty = 0.05	0.02	0.12	89	2400
Uncertainty = 0.1	0.03	0.12	87	2338
Uncertainty = 0.4	0.08	0.14	87	2003
Onshore H_{rms}	−0.00	0.07	94	5683
No Offshore H_{rms}	−0.13	0.30	12	−157
Prior	−0.13	0.30	0	0

4.3. Prediction sensitivity to wave-model parameter uncertainty

Alternatively, we could address the prediction errors by considering model errors. The most straightforward error source is probably the choice of the two free parameters (γ and B) that control the wave-breaking process (Fig. 2). Others have shown that the optimal values of these parameters actually depend on the incident wave conditions and water depth (Apotsos et al., 2008; Ruessink et al., 2003). To account for model-parameter uncertainty, we generated new simulations by varying the wave-breaking parameters uniformly (γ = 0.17 to 0.68 and B = 0.4 to 1.6 in increments that were 10% of the original values), choosing one combination of parameters at a time and re-running the wave model for each of the points in the 20-year time series. This resulted in a total of 1,334,017 simulations that were then used to re-train a Bayesian network, modified to include the model parameters as inputs.

Then, the Duck94 data set was used to update and evaluate the Bayesian-network predictions. Because it has been shown that the optimal values of the two model parameters are correlated (Roelvink and Broker, 1993), we chose to only allow uncertainty in the breaking parameter, γ, and we constrained the other parameter at the original value (B = 0.8). The Bayesian network has, presumably, learned the correlation between the model parameters; it should be able to cope with this constraint. The resulting skill, error, and likelihoods from this sensitivity study are shown in Table 1. The best prediction of the nearshore wave height was obtained when the uncertainty in γ was equal to 0.05 (1 standard deviation), or about 10% of the original parameter value (0.34). The mean and rms wave-height errors were

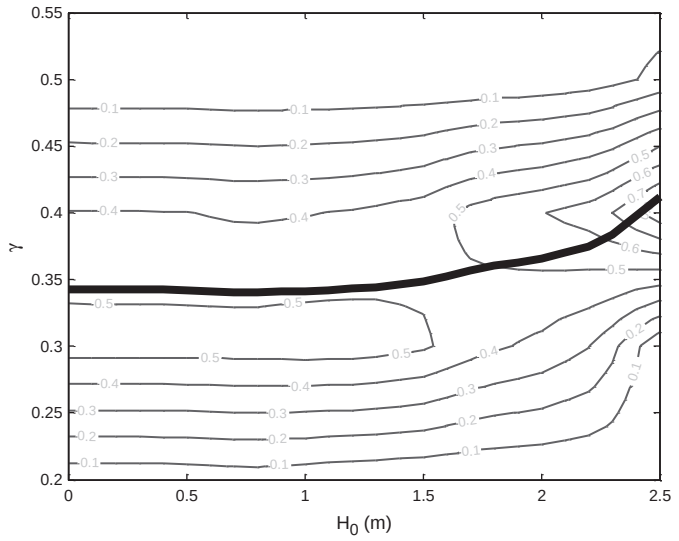

Fig. 11. Probability distribution (contours) and mean value (heavy solid line) of Bayesian estimate of the wave-breaking parameter value (γ) vs. offshore wave height.

lower, and the skill and likelihood ratios were higher than any other choice of uncertainty values applied to γ. We tried some scenarios where both bathymetric and γ uncertainties were allowed (not shown), and these did no better than simply allowing γ uncertainty.

Fig. 10d shows the prediction result for the best-performing scenario with lowest rms wave-height error, highest skill, and highest likelihood ratio. There is considerably more variability in the wave-height prediction uncertainty, compared to the previous examples. This can be attributed to the addition of the wave parameters (γ and B), leading to an increase in the model complexity as well as explicitly acknowledging them as sources of uncertainty. The resulting wave-height prediction uncertainty was higher at times when the actual prediction error was higher; hence, the inclusion of model-parameter uncertainty not only improved the prediction, but also yielded a more accurate error estimate. Specifically, when the original model failed to predict the largest waves, the modified model either improved that prediction (e.g., period between 15 and 16 October) or updated the uncertainty such that it included the observations (e.g., the period between 17 and 19 October). Note also that the smallest wave conditions at the beginning of the analysis period were also better predicted.

The wave-breaking parameter was allowed mild uncertainty such that the input was normally distributed with a mean of 0.34 (the prior) and standard deviation of 0.05. This allowed the Bayesian network to attempt to predict an updated parameter value based on the offshore wave height, period, direction, and water depths. Fig. 11 shows the sensitivity of the estimated value of g that corresponded to the nearshore wave-height predictions shown in Fig. 10d. Under low wave heights (less than about 1.25 m), the most probable value of γ is about 0.3, but the confidence is not very high (probability ~50%) and a value of 0.4 is nearly equally likely. However, as the wave height increased, the optimal value of γ also increased. For wave heights exceeding 2 m, the optimal value of γ is 0.4 or higher. And, under high waves, the parameter uncertainty decreased (indicated by a probability increase), indicating that parameter uncertainty is relatively unimportant under low wave heights and becomes important when wave breaking is important. This dependence on wave height has been demonstrated by others (Apotsos et al., 2008; Roelvink and Broker, 1993; Ruessink et al., 2003). Unlike other efforts to estimate the optimal parameter values, in our implementation, the prior estimate ($\gamma = 0.34$) continues to constrain the updated estimate because we do not allow large uncertainties in this parameter. In Part II, we explore the problem of inverse modeling and the impact of loosening this constraint.

5. Conclusions

We demonstrate that results obtained from a detailed forward model of surf-zone wave evolution are reproduced accurately using a Bayesian-network modeling approach. We tested the Bayesian network using both simplified scenarios and then a real-world prediction example. In the real-world surf-zone example, prediction skill was about 80% if the model inputs (offshore wave conditions, bathymetry, and free parameters) were assumed to be perfect. Using both simplified scenarios and the real-world prediction example, we show that uncertainty in the input data is accurately transferred to uncertainty in the predictions. However, if uncertainties in the boundary and forcing data were not conveyed to the Bayesian network, overly optimistic prediction uncertainties were computed. More skillful prediction uncertainties were obtained by including measured alongshore bathymetric variability as a source of input uncertainty, but prediction skill under this scheme improved only marginally. Alternatively, if model-parameter uncertainty is included, the prediction skill increased substantially (to about 90%), mean and rms errors were reduced, and the predicted uncertainties were more consistent with the observations. The Bayesian network has several advantages. It significantly reduces the dimensionality of the problem, compared to a detailed model; uncertainty estimates are made for all predictions, and it is possible to estimate model parameters simultaneously with making the wave-height prediction.

Acknowledgments

This work was supported by the Office of Naval Research (PE Number: 0602435N for KTH and N0001409IP20080 for NGP). We are indebted to the researchers at the Field Research Facility (Duck, NC) who collected the long time series of bathymetry and wave conditions used in our models. This debt is extended again to the FRF researchers and to Drs. Guza, Gallagher, Herbers, Raubenheimer, and Elgar who collected the Duck94 field observation used to test our predictions. That effort was supported by the Office of Naval Research and the National Science Foundation. Also, we are grateful to Sarah Rennie and Alan Brandt, who introduced us to Bayesian networks and worked with us for several years to develop and understand the potential applications of this approach. Comments from reviews by Drs. P. Howd and A. Reniers led to substantial improvements of this work. Barbara Lidz provided numerous comments that improved the manuscript's clarity.

References

Apotsos, A., Raubenheimer, B., Elgar, S., Guza, R.T., 2008. Testing and calibrating parametric wave transformation models on natural beaches. Coastal Engineering 55, 224–235.

Bell, P.S., 1999. Shallow water bathymetry derived from an analysis of X-band marine radar images of waves. Coastal Engineering 37, 513–527.

Benett, A.F., 2002. Inverse Modeling of the Ocean and Atmosphere. Cambridge University Press.

Birkemeier, W.A., Thornton, E.B., 1994. The DUCK94 nearshore field experiment. In: Arcilla, A.S., Stive, M.J.F., Kraus, N.C. (Eds.), Proc. Coastal Dynamics '94. ASCE, Barcelona, pp. 815–821.

Booij, N., Ris, R.C., Holthuijsen, L.H., 1999. A third generation wave model for coastal region: 1. Model description and validation. Journal of Geophysical Research 104 (c4), 7649–7666.

Chen, Q., Kirby, J.T., Dalrymple, R.A., Shi, F., Thornton, E.B., 2003. Boussinesq modeling of longshore currents. Journal of Geophysical Research 108 (C11). doi:10.1029/2002JC001308.

Elgar, S., Guza, R.T., Raubenheimer, B., Herbers, T.H.C., Gallagher, E.L., 1997. Spectral evolution of shoaling and breaking waves on a barred beach. Journal of Geophysical Research 102 (c7), 15797–15805.

Feddersen, F., Guza, R.T., Elgar, S., 2004. Inverse modeling of one-dimensional setup and alongshore current in the nearshore. Journal of Physical Oceanography 34, 920–933.

Gallagher, E., Guza, R.T., Elgar, S., 1998. Observations of sand bar evolution on a natural beach. Journal of Geophysical Research 103 (C2), 3203–3215.

Haines, J.W., Sallenger Jr., A.H., 1994. Vertical structure of mean cross-shore currents across a barred surf zone. Journal of Geophysical Research 99 (C7), 14,223–14,242.

Henderson, S., Allen, J., Newberger, P., 2004. Nearshore sandbar migration predicted by an eddy-diffusive boundary layer model. Journal of Geophysical Research 109 (C6), C06024.
Hsu, T.-J., Elgar, S., Guza, R.T., 2006. Wave-induced sediment transport and onshore sandbar migration. Coastal Engineering 53, 817–824.
Ihlera, A.T., Kirshner, S., Ghilc, M., Robertsone, A.W., Smytha, P., 2007. Graphical models for statistical inference and data assimilation. Physica D 230, 72–87.
Kurapov, A.L., Egbert, G.D., Allen, J.S., Miller, R.S., 2007. Representer-based variational data assimilation in a nonlinear model of nearshore circulation. Journal of Geophysical Research 112 (C11019). doi:10.1029/2007JC004117.
Lesser, G.R., Roelvink, J.A., van Kestera, J.A.T.M., Stelling, G.S., 2004. Development and validation of a three-dimensional morphological model. Coastal Engineering 51, 883–915.
Norsys, 1990–2007. Netica. Www.norsys.com, Ver. 3.25.
Ooyama, K.V., 1987. Scale-controlled objective analysis. Monthly Weather Review 115, 2479–2506.
O'Reilly, W.C., Guza, R.T., 1998. Assimilating coastal wave observations in regional swell predictions. Part 1: inverse methods. Journal of Physical Oceanography 28 (4), 679–691.
Plant, N.G., Holman, R.A., Freilich, M.H., Birkemeier, W.A., 1999. A simple model for interannual sandbar behavior. Journal of Geophysical Research, Oceans 104 (C7), 15755–15776.
Plant, N.G., Holland, K.T., Puleo, J.A., 2002. Analysis of the scale of errors in nearshore bathymetric data. Marine Geology 191, 71–86.
Plant, N.G., Holland, K.T., Puleo, J.A., Gallagher, E.L., 2004. Prediction skill of nearshore profile evolution models. Journal of Geophysical Research 109 (C01006). doi:10.1029/2003JC001995.
Plant, N.G., Holland, K.T., Holman, R.A., 2006. A dynamical attractor governs beach response to storms. Geophysical Research Letters 33 (L17607). doi:10.1029/2006GL027105.
Plant, N.G., Edwards, K.L., Kaihatu, J.M., Veeramony, J., Hsu, L., Holland, K.T., 2009. The effect of bathymetric filtering on a nearshore process model. Coastal Engineering 56, 484–493.
Reniers, A.J.H.M., MacMahan, J.H., Thornton, E.B., Stanton, T.P., 2007. Modeling of very low frequency motions during RIPEX. Journal of Geophysical Research 112 (cc07013). doi:10.1029/2005JC003122.
Ris, R.C., Holthuijsen, L.H., Booij, N., 1999. A third generation wave model for coastal regions: 2. Verification. Journal of Geophysical Research 104 (c4), 7667–7681.
Roelvink, J.A., Broker, I., 1993. Cross-shore profile models. Coastal Engineering 21 (1–3), 163–191.
Ruessink, B.G., Kroon, A., 1994. The behavior of a multiple bar system in the nearshore zone of Terschelling, the Netherlands, 1965–1993. Marine Geology 121, 187–197.
Ruessink, B.G., Walstra, D.J.R., Southgate, H.N., 2003. Calibration and verification of a parametric wave model on barred beaches. Coastal Engineering 48, 139–149.
Ruessink, B.G., Kuriyama, Y., Reniers, A.J.H.M., Roelvink, J.A., Walstra, D.J.R., 2007. Modeling cross-shore sandbar behavior on the timescale of weeks. Journal of Geophysical Research 112 (F03010). doi:10.1029/2006JF000730.
Thornton, E.B., Guza, R.T., 1983. Transformation of wave height distribution. Journal of Geophysical Research 88 (C10), 5925–5938.
van Dongeren, A., Plant, N., Cohen, A., Roelvink, D., Haller, M.C., Catalán, P., 2008. Beach Wizard: nearshore bathymetry estimation through assimilation of model computations and remote observations. Coastal Engineering 55 (12), 1016–1027.
Westerink, J.J., Luettich, R.A., Feyen, J.C., Atkinson, J.H., Dawson, C., Roberts, H.J., Powel, M.D., Dunion, J.P., Kubatko, E.J., Pourtaher, H., 2008. A Basin- to Channel-Scale Unstructured Grid Hurricane Storm Surge Model Applied to Southern Louisiana. Monthly Weather Review 136, 833–864. doi:10.1175/2007MWR1946.1.
Wijnberg, K.M., Terwindt, J.H.J., 1995. Extracting decadal morphological behavior from high-resolution, long-term bathymetric surveys along the Holland coast using eigenfunction analysis. Marine Geology 126, 301–330.
Wikle, C.K., Berliner, L.M., 2007. A Bayesian tutorial for data assimilation. Physica D 230, 1–16.
Wright, L.D., Short, A.D., Green, M.O., 1985. Short-term changes in the morphodynamic states of beaches and surf zones: an empirical predictive model. Marine Geology 62, 339–364.